Progress In Electromagnetics Research C, Vol. 91, 213–225, 2019

A New Approximation for Calculating the Attraction Force in Cylindrical Permanent Magnets Arrays and Cylindrical Linear Single-Axis-Actuator

Naamane Mohdeb*, Hicham Allag, and Tarik Hacib

Abstract—New accurate approximation is proposed using integral expressions for evaluating the magnetic force between cylindrical permanent magnet arrays. The magnetic field distribution is calculated analytically by using Coulombian model. In this paper, every cylindrical magnet is divided into elementary cuboidal magnets. The accuracy can be controlled by regulating the value of elementary cuboidal permanent magnets "N". The approximation can also be used to calculate the force interaction in the cylindrical linear single-axis-actuator. We confirm the validity of magnetic force calculation by comparing it with other methods and measurements. The calculation results are in very good agreement with measured values, which indicates the feasibility of our approximation.

1. INTRODUCTION

In some applications, such as eddy current dampers, magnetic refrigerators, micropumps, the calculation of interaction force, torque and field is very important [1–4].

The benefit for these applications is that magnetic forces act without physical contact over larger distances than electrostatic, piezoelectric or other schemes [5, 8, 9]. In the literature related to permanent magnets, calculations of forces between magnets of various shapes and geometries have their relevance in the context of several applications. For investigating the magnetic force between two sets of cylindrical permanent magnets (Fig. 1), the force engendered between two parallel magnets should be calculated firstly.

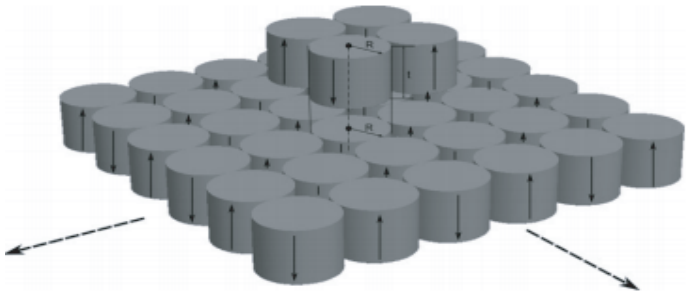

Figure 1. A scheme of two sets of cylindrical magnets.

The analytical expression of the attractive force between two arrays of cylindrical permanent magnets was derived from the derivative of the total magnetostatic interaction energy with respect

Received 8 January 2019, Accepted 19 March 2019, Scheduled 2 April 2019
* Corresponding author: Naamane Mohdeb (mohdeb.naamane@gmail.com).
The authors are with the L2EI, Université de Jijel, BP 98, OuledAissa 18000, Algeria.

to the axial coordinate [5, 6]. Calculating the force is a very complex procedure, as it depends on the form, magnetization, and orientation of the magnets.

Several expressions for the force between cylindrical magnets have also been published in previous literature [7–17], and they did not make use of exact solutions in any form and are more complex than the expression to be presented in the current work. The magnetic field produced by a cylindrical permanent magnet can be determined with the same analytical formulation as the one used for a cylindrical thin coil [9].

The Green formula was used to derive the analytical equations for magnetic field generated by cylindrical coil, and the correlation between the cylindrical coil and axially magnetized permanent magnet of annular shape is achieved [18, 19]. Agashe and Arnold presented analytical formula based on the assumption of uniform magnetization in the axial direction while using a magnetic field approximation for a cylindrical magnet [14]. The analytical expressions are complex and computationally more expensive than the closed form expression given by Furlani et al. [15–17]. Ravaud et al. [9] have given elliptic integrals without any simplification for magnetic parameters such as field, force, torque, and stiffness in cylindrical magnets and coil.

The interactions between cylindrical magnets are established by multiple integrals in polar coordinates. In this paper, we use new approximation to solve this problem. For calculating the magnetic field created by cylindrical magnets, analytical expressions will be proposed by us. The expressions can be used to calculate the force between two sets of magnets in a computationally efficient way. Also, these analytical expressions will be used to evaluate the magnetic interactions in cylindrical linear single axis-actuator.

2. PROBLEM FORMULATION

Figure 2 shows that the magnetic configuration consists of two magnets with axial polarization. The dimensions of the system are shown in Fig. 2. $2a$ and $2A$ are the radii of magnet 1 and magnet 2. $2C$ and $2c$ are the thicknesses of the magnets. The cylinder shown in Fig. 2 is uniformly magnetized in the z direction.

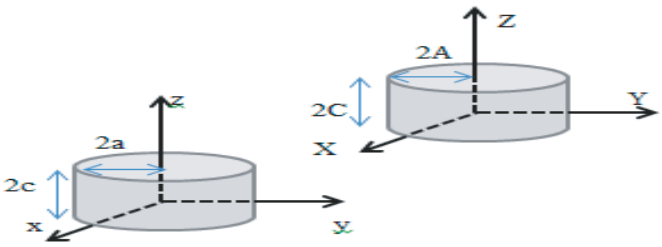

Figure 2. Two cylindrical magnets with parallel magnetization.

2.1. Magnetic Vector Potential and Magnetic Flux Density of Cylindrical Magnets

The modeling of magnets can be based on Coulombian method, and the Coulombian approach replaces the magnet by two surfaces distribution of fictitious magnetic charge with surface density $\sigma* = M \cdot \mathbf{n}$ [20], where M is the magnetization, and $\mathbf{n}$ is the unit vector normal to the surface. Fig. 3 shows a rectangular permanent magnet with uniform magnetization in the z-direction.

For circular surface, we can approximate circle with several rectangles. We will approximate the graph by dividing the interval into "n" subintervals, each of width, $\Delta x = (2a)/n$. The rectangle height is established by evaluating the values of $f(c)$, as shown for the typical case $x = c$, where the rectangle height is $f(c)$.

In Fig. 4, we approximate the surface using inner rectangles (each rectangle is inside the curve). We can then find the region of each of these rectangles and add them up, and this will be an estimate of the region.

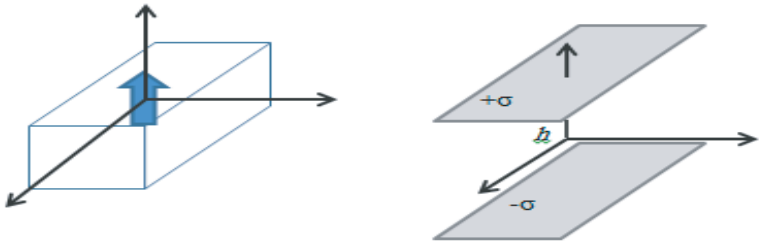

Figure 3. Model of the permanent magnet by the Coulombian approach.

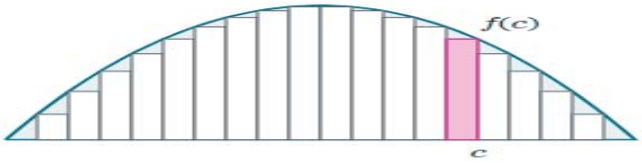

Figure 4. Approximating area under a curve using rectangles.

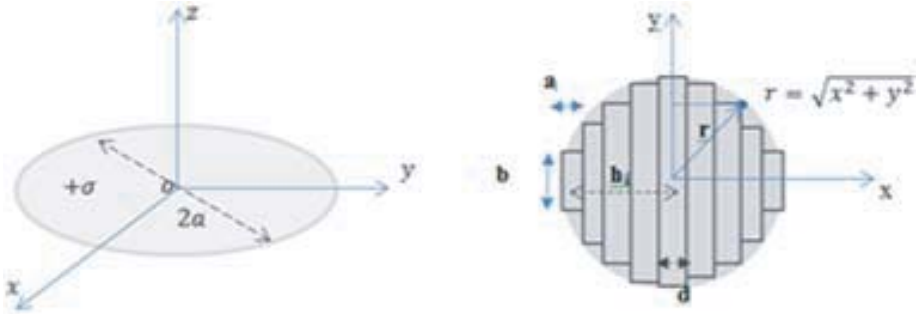

Figure 5. Decomposition of the circular surface in rectangular element.

Using several rectangles will give us an exact approximation of the circular surface. The size of the rectangular elements is $2a \times 2b$, and "h_i" is the center of each element.

To calculate the magnetic force magnetic between cylindrical magnets, we should first calculate the scalar magnetic potential resulting from one of the circular surfaces (Fig. 5) and any given point P (arbitrary observation point) [23–25]. The potential can be calculated by the formula:

$$\varphi_e(R) = \frac{1}{4\pi\mu_0} \iint_S \frac{\sigma}{R_e} dS_e \tag{1}$$

$$R_e = \sqrt{(\alpha - h_{ex} - x_e')^2 + (\beta - h_{ey} - y_e')^2 + (\gamma - h_{ez} - z')^2} \tag{2}$$

where R_{eij} is the distance between the source point (x_e', y_e', z') in rectangular element and observation point P $(\alpha, \beta, \gamma.)$ The coordinate marked by "e" is related to the source. With suitable substitutions for dS_e, the following equation for scalar magnetic potential is obtained:

$$\varphi_e(R) = \frac{1}{4\pi\mu_0} \int_{-a}^{a} \int_{-b}^{b} \frac{\sigma}{R_e} dx_e' dy_e' \tag{3}$$

If we substitute R then Eq. (2) becomes

$$\varphi_e = \frac{1}{4\pi\mu_0} \int_{-U_e}^{U_e} \int_{-V_e}^{V_e} \frac{\sigma}{\sqrt{U_e^2 + V_e^2 + W^2}} dU_e dV_e \tag{4}$$

where

$$\begin{aligned} U_e &= (\alpha - h_{ex}) - x_e{}' \\ V_e &= (\beta - h_{ey}) - y_e' \\ W &= (\gamma - h_{ez}) - z' \\ R_e &= \sqrt{U_e^2 + V_e^2 + W^2} \end{aligned} \tag{5}$$

The total scalar potential becomes

$$\varphi_t = \frac{\sigma}{4\pi\mu} \sum_{e=1}^{N} \sum_{i=0}^{1} \sum_{j=0}^{1} (-1)^{i+j} \cdot \varphi_e \tag{6}$$

where

$$\varphi_e = -U_e \ln (R_e - V_e) - V_e \ln (R_e - U_e) \operatorname{Warctg} \left(\frac{U_e V_e}{R_e W} \right) \tag{7}$$

By adding the field created by the two surfaces, we obtain the field created by an elementary cuboidal magnet (Fig. 6). The system of magnet is shown in Fig. 6, in which the cylindrical magnet is replaced by cuboidal shape composed of N cuboidal magnets.

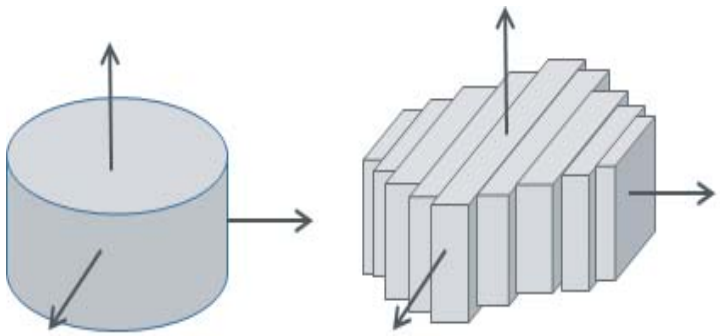

Figure 6. Elementary decomposition of cylindrical magnet in cubic elements.

The total magnetic field is always calculated from the gradient:

$$B_{xt} = \frac{J}{4\pi} \sum_{e=1}^{N} \sum_{i=0}^{1} \sum_{j=0}^{1} \sum_{k=0}^{1} (-1)^{i+j+k} \log(R_e - V_e) \tag{8}$$

$$B_{yt} = \frac{J}{4\pi} \sum_{e=1}^{N} \sum_{i=0}^{1} \sum_{j=0}^{1} \sum_{k=0}^{1} (-1)^{i+j+k} \log(R_e - U_e) \tag{9}$$

$$B_{zt} = \frac{J}{4\pi} \sum_{e=1}^{N} \sum_{i=0}^{1} \sum_{j=0}^{1} \sum_{k=0}^{1} (-1)^{i+j+k} \operatorname{arctg} \left(\frac{U_e V_e}{R_e W_e} \right) \tag{10}$$

where

$$\begin{aligned} U_e &= (\alpha - h_{ex}) - (-1)^i a \\ V_e &= (\beta - h_{ey}) - (-1)^j b \\ W_e &= (\gamma - h_{ez}) - (-1)^k c \\ R_e &= \sqrt{U_e^2 + V_e^2 + W_e^2} \end{aligned} \tag{11}$$

In Fig. 7, we present the magnetic flux density created by cylindrical magnet for the number of subdivisions: $N = 4$ and $N = 40$.

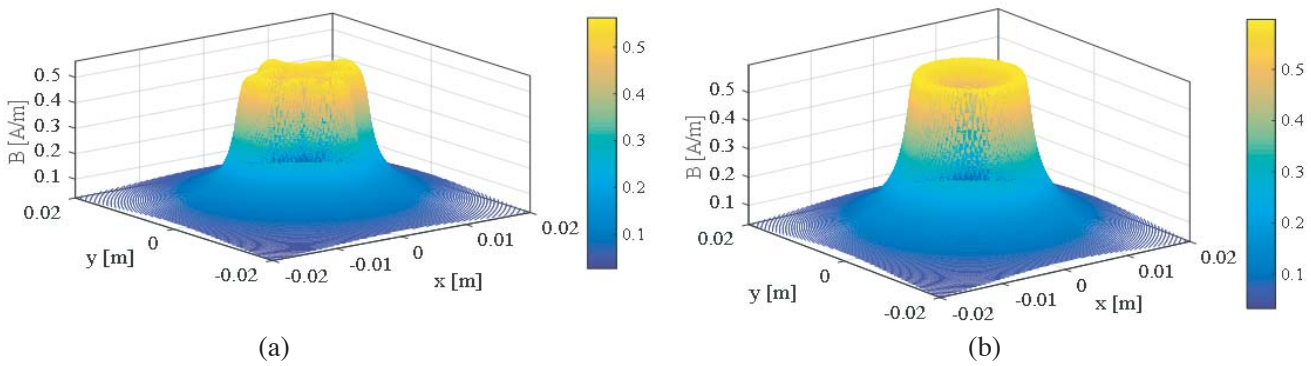

Figure 7. The magnetic flux density in XY plane for (a) $N = 4$ elements, (b) $N = 40$ elements.

The permanent magnet shape is set to be cylinder, in which bottom diameter $d = 1\,\text{mm}$, height $h = 10\,\text{mm}$, and residual flux density $B_m = 1.15\,\text{T}$. The cylinder center is the origin, and the central axis of the permanent magnet is z-axis (the positive direction is the direction of N pole). The magnetic flux density distribution of permanent magnet according to the number of decomposition N is shown in Fig. 7. When increasing the number of elements one arrives at the exact geometry of cylindrical magnet, which shows that this approach has a remarkable efficiency. The accuracy with the method can be controlled by adjusting the value of N.

The comparison between the magnetic field calculation and the measured values when the sensors move along the z-direction is shown in Fig. 8.

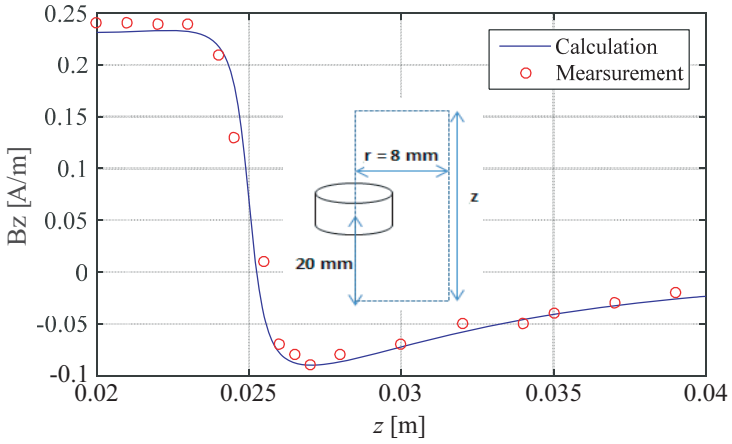

Figure 8. Magnetic induction B_z obtained from measurement and our results.

2.2. Analytical Calculation of the Magnetic Field Created by Annular Permanent Magnet

In this section, we compare the results determined by our approximation of magnetic field strength created by an annular permanent magnet, whose magnetization is in the z-direction, using results from those obtained in [18]. Using superposition principle (Fig. 9), the magnetic field created by annular permanent magnet can be calculated more easily with our 3D approximation.

In Fig. 10 we show the radial components of magnetic field as a function of the radial distance of the observation point for a given altitude with $z = 3\,\text{mm}$. Fig. 10 shows that the results are in agreement with integral expression.

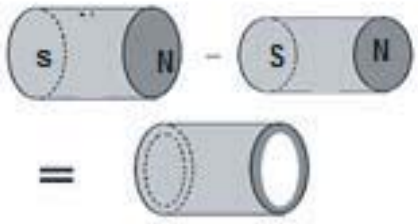

Figure 9. Modeling of permanent magnet annular Superposition principle.

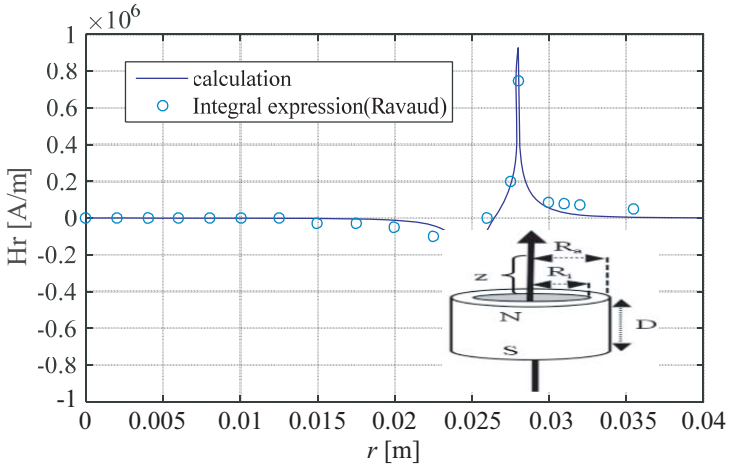

Figure 10. Field radial component versus the radial distance r of the observation point; $D = 3\,\text{mm}$, $R_i = 25\,\text{mm}$, $R_a = 28\,\text{mm}$.

2.3. Calculation of Interaction Forces between Cylindrical Magnets

For the calculation of interaction forces between two cylindrical magnets, we divided the first and second into (N, M) elementary cuboidal magnets. The interaction energy between two elementary magnets t and s, as shown in Fig. 11, is given by

$$E_{t,s} = \frac{JJ'}{4\pi\mu} \sum_{p=0}^{1} \sum_{q=0}^{1} (-1)^{p+q} \cdot \int_{-B}^{B} \int_{-A}^{A} \int_{-b}^{b} \int_{-a}^{a} \frac{1}{R} dx dy dX dY \tag{12}$$

From the interaction energy, the force components can be obtained by

$$\vec{F_{s,t}} = gr\vec{a}d(E_{s,t}) \tag{13}$$

For the three components of force,

$$F_{s,t} = \frac{JJ'}{4\pi\mu} \sum_{s=1}^{N} \sum_{t=1}^{M} \sum_{i=0}^{1} \sum_{j=0}^{1} \sum_{k=0}^{1} \sum_{l=0}^{1} \sum_{p=0}^{1} \sum_{q=0}^{1} (-1)^{i+j+k+l+p+q} \cdot \psi_{st(x,y,z)} \tag{14}$$

with

$$\psi_{stx} = \frac{1}{2}\left(V_{st}^2 - W_{st}^2\right) \ln\left(R_{st} - U_{st}\right) + U_{st}V_{st} \ln\left(R_{st} - V_{st}\right) + V_{st}W_{st} \arctan\left(\frac{U_{st}V_{st}}{R_{st}W_{st}}\right) + \frac{1}{2}R_{st}U_{st} \tag{15}$$

$$\psi_{sty} = \frac{1}{2}\left(U_{st}^2 - W_{st}^2\right) \ln\left(R_{st} - V_{st}\right) + U_{st}V_{st} \ln\left(R_{st} - U_{st}\right) + U_{st}W_{st} \arctan\left(\frac{U_{st}V_{st}}{R_{st}W_{st}}\right) + \frac{1}{2}R_{st}V_{st} \tag{16}$$

$$\psi_{stz} = -U_{st}W_{st} \ln\left(R_{st} - U_{st}\right) - W_{st}V_{st} \ln\left(R_{st} - V_{st}\right) + U_{st}W_{st} \arctan\left(\frac{U_{st}V_{st}}{R_{st}W_{st}}\right) - R_{st}W_{sk} \tag{17}$$

The intermediate variables appearing in Eq. (17) are

$$\begin{aligned} U_{st} &= \alpha + (A(s+1) - 2i\Delta x2_s(s)) - (a(t+1) - 2j\Delta x1_t(t)) \\ V_{st} &= \beta + (-1)^p B(s) - (-1)^l b(t) \\ W_{st} &= \gamma + (-1)^q C - (-1)^k c \\ \Delta x1_s(s) &= ((A(s+1) - A(s))/2 \\ \Delta x2_t(t) &= ((a(t+1) - a(t))/2 \\ R_{st} &= \sqrt{U_{st}^2 + V_{st}^2 + W_{st}^2} \end{aligned} \tag{18}$$

As shown in Fig. 11, the dimensions of the first elementary cuboidal magnet are a, b, and c, and its polarization is J. For the second elementary magnet, the dimensions are A, B and C. Its polarization is J', and the coordinate of its center is α, β, and γ. $\Delta x1_s$ and $\Delta x2_t$ are the widths of the first and second elementary magnets.

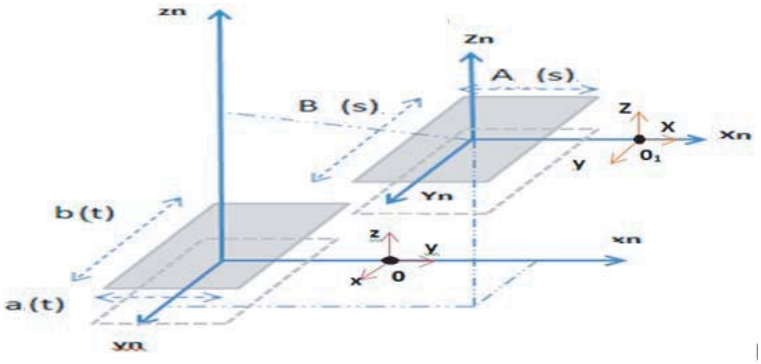

Figure 11. System of two rectangular elements.

The upper magnet moves in translation along the y-axis above the lower fixed magnet. The total magnetic force is given by:

$$F_{magnet} = \sum_{s=1}^{N} \sum_{t=1}^{M} F_{s,t} \tag{19}$$

where N and M are the number of first and second elementary magnets, respectively.

To verify the validity of the analytical results, the force between two magnets was calculated. Fig. 12 shows the force distribution, and we notice that the force in the direction is in a sinusoidal form

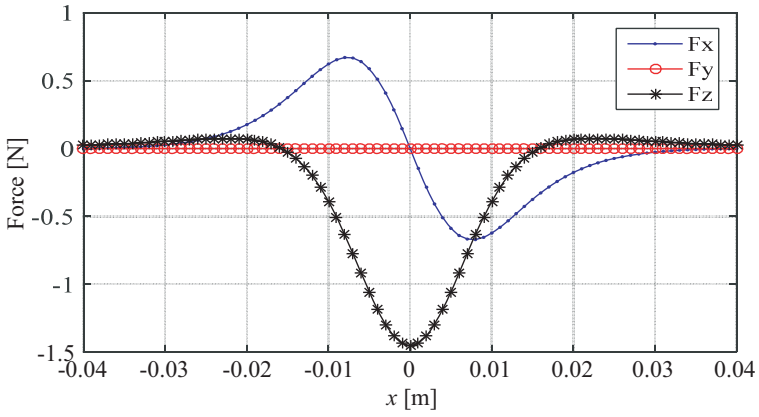

Figure 12. Force components for $t = 10\,\text{mm}$, $r = 10\,\text{mm}$ and $x = 10\,\text{mm}$.

whose positive part is in the negative direction of the movement. This phenomenon repeats itself but in the opposite direction because of the symmetry of displacement. On the other hand, the force along the axis 'oz' reaches the maximum value when the two magnets are in quadrature. The force along the axis 'ox' is always zero.

Figure 13 shows variation of the force versus axial distance between the two cylindrical magnets. We can see that the calculation describes the experimental behavior fairly well.

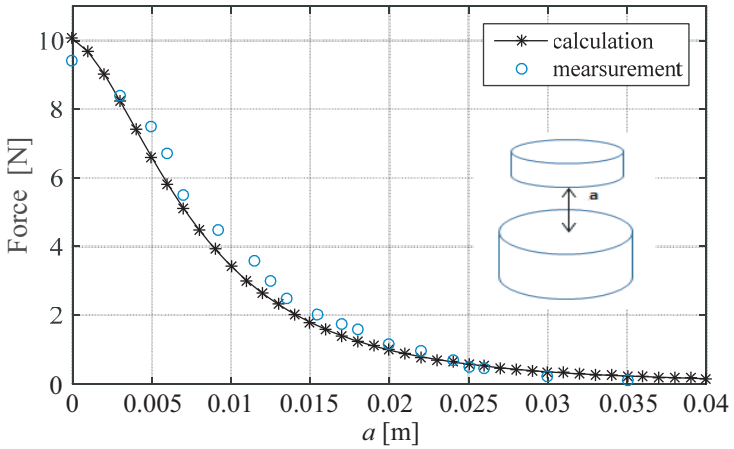

Figure 13. Force between the two cylindrical magnets versus the axial axis.

2.4. Attraction Magnetic Force Determination between Two Sets of Cylindrical Magnets

Permanent magnets may be grouped into arrays to adjust their mutual interaction and consequently, the force acting upon them [5]. Recently, permanent magnet arrays have been utilized in many applications; among others: eddy current dampers magnetic refrigerators and micropumps [5–7].

In this section, we determine the magnetic force among three sets containing 2×2, 4×4, and 6×6 magnets, axially magnetized permanent magnets with alternating orientation of magnetization within

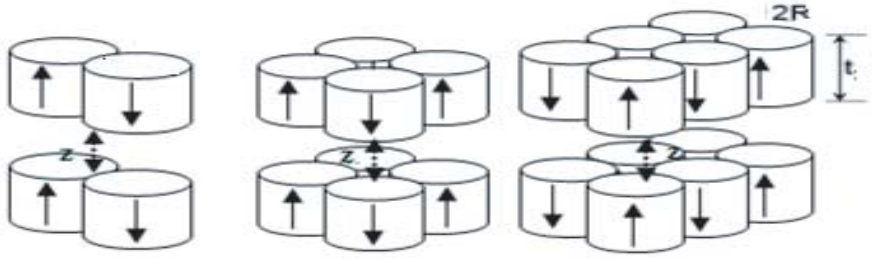

Figure 14. A Scheme of three sets of cylindrical magnets; $R = 2\,\text{mm}$ and $t = 8\,\text{mm}$.

Table 1. Comparison of magnetic force (magnet set 4×4).

Force (N)	Measurement	Our results
F (z =0)	9.550	9.400
F ($z = 0.5e-3$)	5.110	5.493
F ($z = 10e-3$)	0.320	0.295
F ($z = 14.8e-3$)	0.100	0.118

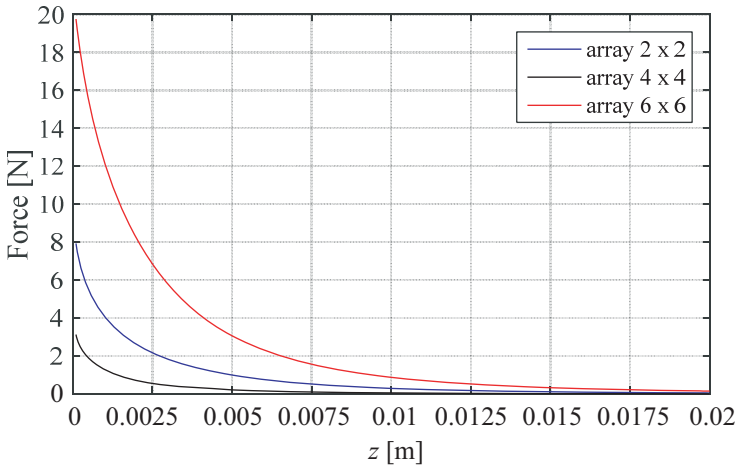

Figure 15. Calculated data for attraction force between three magnet set (2×2), (4×4) and (6×6).

the arrays (Fig. 14). Fig. 15 shows calculated data for the attraction force between three magnet sets (2×2), (4×4), and (6×6) for various vertical displacements.

Comparison of results for the normalized levitation magnetic force of two cylindrical permanent magnets, obtained using the presented approach and the measurements values versus z-axis for parameters $R = 3\,\text{mm}$ and $t = 1.5\,\text{mm}$, are given in Table 1.

2.5. Magnetic Field and Force in Cylindrical Single-axis Actuator

The force formula between cylindrical magnets can also be used to evaluate the force between thin coils and magnet. The fastest way to calculate forces in the cylindrical linear single-axis actuator [21, 26–28] is to use the Lorenz force calculations, as the estimation of the magnetic field of the coils is not necessary [21, 22]. The structure is shown in Fig. 16(a). The coil is modeled by four straight bars, as shown in Fig. 16(b), where each bar is defined by dimensions $2a \times 2b \times 2c$.

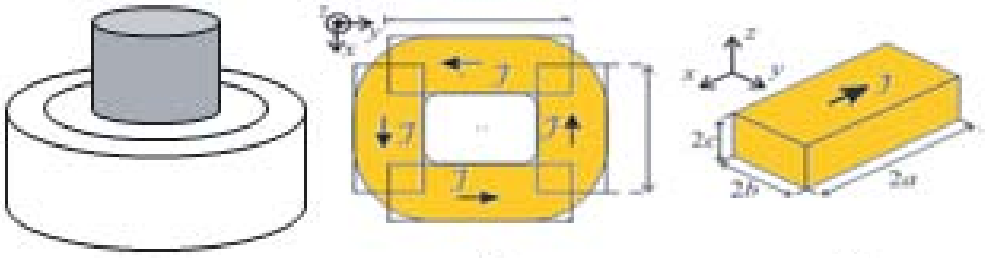

Figure 16. (a) System composed of a permanent magnet and thin coil. (b) The coil is replaced by four bars). (c) Bar-shaped volume current density.

The total magnetic force acting on the thin coil is given by

$$\vec{F_T} = \int_{V_c} \vec{J_c} \times \vec{B} dV_c \tag{20}$$

$$\vec{F_T} = \int_{V_c} \begin{pmatrix} Jx \\ Jy \\ 0 \end{pmatrix} \times \begin{pmatrix} B_{xt} \\ B_{yt} \\ B_{zt} \end{pmatrix} dX dY dZ \tag{21}$$

where V_c is the volume of the bar-shaped volume. J_c is the current density in bar-shaped volume, and B is the field created by a cylindrical magnet.

By representing the coil as four overlapping straight beams (Fig. 16(b)), the magnetic force has been obtained analytically. The force is derived for the bar-shaped volume shown in Fig. 16(c), with volume current density J and dimension $(2A \times 2B \times 2C)$.

The coil moves in translation along the z direction. The interaction force between the coil and cylindrical magnet is given by Eqs. (22)–(25).

The current in x-direction (Fig. 17(a))

$$F_y = -\frac{I}{CB}\frac{B}{4\pi}\sum_{t=1}^{M}\sum_{i}\sum_{j}\sum_{k}\sum_{l}\sum_{p}\sum_{q}(-1)^{i+j+k+l+p+q}\varphi_n \tag{22}$$

$$F_z = \frac{I}{CB}\frac{B}{4\pi}\sum_{t=1}^{M}\sum_{i}\sum_{j}\sum_{k}\sum_{l}\sum_{p}\sum_{q}(-1)^{i+j+k+l+p+q\psi_n} \tag{23}$$

The current in y-direction (Fig. 17(b))

$$F_x = -\frac{I}{CA}\frac{B}{4\pi}\sum_{t=1}^{M}\sum_{i}\sum_{j}\sum_{k}\sum_{l}\sum_{p}\sum_{q}(-1)^{i+j+k+l+p+q}\varphi_n \tag{24}$$

$$F_z = \frac{I}{CA}\frac{B}{4\pi}\sum_{t=1}^{M}\sum_{i}\sum_{j}\sum_{k}\sum_{l}\sum_{p}\sum_{q}(-1)^{i+j+k+l+p+q}\phi_n \tag{25}$$

The forces are obtained with the intermediate variables which are given by

$$\begin{aligned}\varphi_n &= \iiint \operatorname{arctg}\left(\frac{VU}{WR}\right)dXdYdZ = \frac{R}{6}\left(U^2+V^2-W^2\right)+6UVW\operatorname{arctg}\left(\frac{VU}{WR}\right)\\ &\quad -3U\left(V^2-W^2\right)\operatorname{arctg}h\left(\frac{R}{V}\right)-3V\left(U^2-W^2\right)\operatorname{arctg}h\left(\frac{R}{V}\right)\Big)\end{aligned} \tag{26}$$

$$\begin{aligned}\phi_n &= \iiint \log\left(-V+R\right)dXdYdZ = \frac{1}{36}\Big(-24U^3\operatorname{arctg}\left(\frac{V}{U}\right)+12VWR-18U^2W\log(R+V)\\ &\quad -18U^2V\log\left(R+W\right)+36UVW\log\left(R-U\right)+18UW^2\operatorname{arctg}\left(\frac{UV}{WR}\right)+18UV^2\operatorname{arctg}\left(\frac{UW}{VR}\right)\\ &\quad +6W^3\log\left(R+V\right)+6V^3\log\left(R+W\right)+24U^2V-6U^3\operatorname{arctg}\left(\frac{VW}{RU}\right)+18UV^2\operatorname{arctg}\left(\frac{W}{V}\right)\\ &\quad +36UW^2\operatorname{arctg}\left(\frac{V}{W}\right)+18UW^2\operatorname{arctg}\left(\frac{W}{V}\right)-54UVW-2V^3\Big)\end{aligned} \tag{27}$$

$$\begin{aligned}\psi_n &= \iiint \log\left(-U+R\right)dXdYdZ = \frac{1}{36}\Big(-24V^3\operatorname{arctg}\left(\frac{U}{V}\right)+12UWR-18V^2W\log(R+U)\\ &\quad -18V^2U\log\left(R+W\right)+36UVW\log\left(R-V\right)+18VW^2\operatorname{arctg}\left(\frac{UV}{WR}\right)+18VU^2\operatorname{arctg}\left(\frac{VW}{UR}\right)\\ &\quad +6W^3\log\left(R+U\right)+6U^3\log\left(R+W\right)+24V^2U-6V^3\operatorname{arctg}\left(\frac{UW}{RV}\right)+18VVU^2\operatorname{arctg}\left(\frac{W}{U}\right)\\ &\quad +36VW^2\operatorname{arctg}\left(\frac{U}{W}\right)+18VW^2\operatorname{arctg}\left(\frac{W}{U}\right)-54UVW-2U^3\Big)\end{aligned} \tag{28}$$

with

$$\begin{aligned}U &= \alpha+(-1)^i A-\left(a\left(t+1\right)-2j\Delta x1_t\left(t\right)\right)\\ V &= \beta+(-1)^k B-(-1)^l b\left(t\right)\\ W &= \gamma+(-1)^p C-(-1)^q c\\ \Delta x1_t\left(t\right) &= \left(\left(a\left(t+1\right)-a\left(t\right)\right)/2\right.\end{aligned} \tag{29}$$

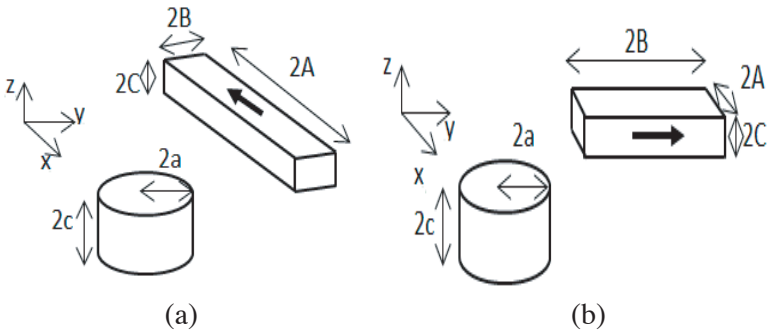

Figure 17. PM and massive conductor in (a) x-direction, (b) y-direction.

Table 2. Design parameters for magnet coil system.

Dimensions	Quantity	Value
I	Coil current	0.2 A
R_c	Outer radius of primary coil	18 mm
r_c	Inner radius of primary coil	14 mm
L_c	Length of primary coil	10 mm
N_c	Number of turns of primary coil	120
α	Distance between coil and magnet in x-direction	0 mm
β	Distance between coil and magnet in y-direction	0 mm
γ	Distance between coil and magnet in z-direction	variable
R_m	Magnet radius	7.5 mm
B_r	Magnet remanence	1 T
L_m	Magnet length	10 mm

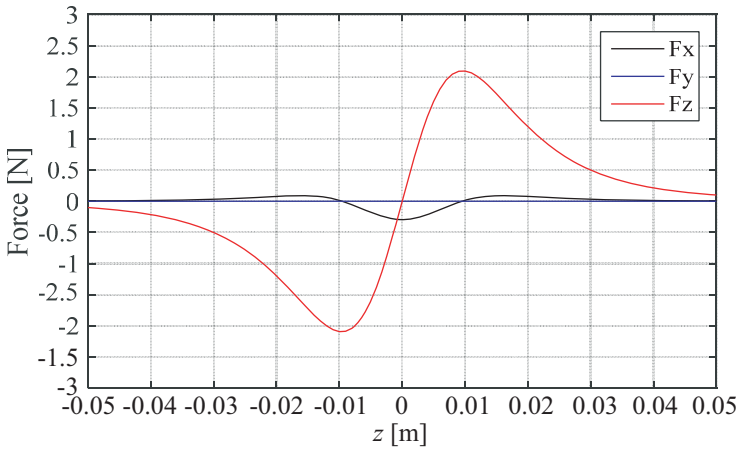

Figure 18. The magnetic induction intensity of force magnetic on the z-axis.

The force acting on the rectangular coil is then equal to the sum of the Lorentz force acting on each of the four volumes. The integrals expression is set up under mathematica environment. The dimensions of the four volumes are shown in Table 2.

An expression for the force between thin coils and magnet has also been published by Robertson et al. It is more complex than the expression to be presented in the current work. In a related work, Xu et al. [27] presented a simplification equation for the axial force between magnet and thin coils, for which further application of their results is required to calculate the forces between coils with many turns,

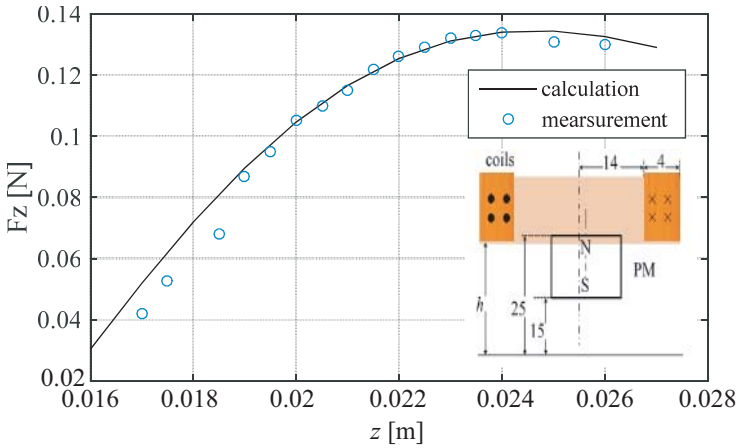

Figure 19. Axial force 'Fz' obtained from measurement and our approximation in different positions.

such as for the system examined here. Here, we calculate the distribution of Lorentz force acting on thin coil.

In Fig. 18, has a zero force when it is axially centered with the magnet. In z-direction, a restoring force is applied by the magnet in the opposite direction of displacement. Fig. 18 shows the interaction force acting on the thin coil obtained from our approximation. Also calculation results have been confirmed by measurement values (Fig. 19). The measurement and simulation results are in very good agreement with calculation that indicates the feasibility of approximation formulas.

3. CONCLUSION

An accurate approximation method for magnetic force calculation between cylindrical magnets sets containing cylindrical magnets and the interaction magnet-thin coil has been presented in this paper. The validity of the method has been verified by the measurement values. The accuracy with the novel approximation can be controlled by regulating the value of elementary cuboidal permanent magnets "N". Results obtained by the new approximation between interaction magnetic force calculation and measurement values are in excellent agreement with the each other.

REFERENCES

1. Zangwill, A., *Modern Electrodynamics*, Cambridge University Press, 2013.
2. Reitz, J. R., F. J. Milford, and R. W. Christy, *Foundations of Electromagnetic*, Addison-Wesley, Wilmington, 1996.
3. Griffiths, D. J., *Introduction to Electrodynamics*, Pearson, Harlow, 2014.
4. Lemarquand, V. and G. Lemarquand, "Passive permanent magnet bearings for rotating shaft: Analytical calculation," *Magnetic Bearings, Theory and Applications*, 85–116, Sciyo Published book, October 2010.
5. Akoun, G. and J. P. Yonnet, "3D analytical calculation of the forces exerted between two cuboidal magnets," *IEEE Transactions on Magnetics*, Vol. 20, No. 5, 1962–1964, 1984.
6. Vokoun, D., M. Beleggia, L. Heller, and P. Sittner, "Magnetostatic interactions and forces between cylindrical permanent magnets," *Journal of Magnetism and Magnetic Materials*, Vol. 321, No. 22, 3758–3763, November 2009.
7. Vokoun, D., G. Tomassetti, M. Beleggia, and I. Stachiv, "Magnetic forces between arrays of cylindrical permanent magnets," *Journal of Magnetism and Magnetic Materials*, Vol. 323, No. 1, 55–60, January 2011.

8. Vokoun, D. and M. Beleggia, "Forces between arrays of permanent magnets of basic geometric shapes," *Journal of Magnetism and Magnetic Materials*, Vol. 350, 174–178, January 2014.
9. Ravaud, R., G. Lemarquand, S. Babic, V. Lemarquand, and C. Akeyel, "Cylindrical magnets and coils: Fields, forces and inductances," *IEEE Transactions on Magnetics*, Vol. 46, 3585–3590, 2010.
10. Ravaud, R., G. Lemarquand, and V. Lemarquand, "Force and stiffness of passive magnetic bearings using permanent magnets. Part 1: Axial magnetization," *IEEE Transactions on Magnetics*, Vol. 45, 2996–3002, 2009.
11. Ravaud, R., G. Lemarquand, and V. Lemarquand, "Force and stiffness of passive magnetic bearings using permanent magnets. Part 2: Radial magnetization," *IEEE Transactions on Magnetics*, Vol. 45, 3334–3342, 2009.
12. MacLatchy, C. S., P. Backman, and L. Bogan, "A quantitative magnetic braking experiment," *American Journal of Physics*, Vol. 61, No. 12, 1096–1101, 1993.
13. Hossein Partovi, M. and E. J. Morris, "Eddy current damping of a magnet moving through a pipe," *Canadian Journal of Physics*, Vol. 84, 253–274, 2006.
14. Agashe, J. S. and D. P. Arnold, "Analytical force calculations and scaling effects for cylindrical and cuboidal micro-magnets," *Intermag. Conf.*, San Diego, CA, May 2006.
15. Furlani, E. P., S. Reznik, and W. Jansen, "A three-dimensional field solution for bipolar cylinders," *IEEE Transactions on Magnetics*, Vol. 30, No. 5, 2916–2919, IEEE, September 1994.
16. Furlani, E. P., "Analytical analysis of magnetically coupled multipole cylinders," *Journal of Physics D: Applied Physics*, Vol. 33, 28–33, 2000.
17. Furlani, E. P., S. Reznik, and A. Kroll, "A three-dimensional field solution for radially polarized cylinders," *IEEE Transactions on Magnetics*, Vol. 31, No. 1, 844–851, 1995.
18. Ravaud, R. G., V. Lemarquand and C. Depollier, "Analytical calculation of the magnetic field created by permanent-magnet rings," *IEEE Transactions on Magnetics*, Vol. 44, No. 8, 1982–1989, August 2008.
19. Ravaud, R., G. Lemarquand, V. Lemarquand, and C. Depollier, "Discussion about the analytical calculation of the magnetic field created by permanent magnets," *Progress In Electromagnetics Research B*, Vol. 11, 281–297, 2009.
20. Rakotoarison, H., J. Yonnet, and B. Delinchant, "Using Coulombian approach for modelling scalar potential and magnetic field of a permanent magnet with radial polarization," *IEEE Transactions on Magnetics*, Vol. 43, 1261–1264, April 2007.
21. Ravaud, R., G. Lemarquand, and V. Lemarquand, "Force and stiffness of passive magnetic bearings using permanent magnets. Part 1: Axial Magnetization," *IEEE Transactions on Magnetics*, Vol. 45, 2996–3002, 2009.
22. Robertson, W., B. Cazzolato, and A. Zander, "A simplified force equation for coaxial cylindrical magnets and thin coils," *IEEE Transactions on Magnetics*, Vol. 47, 2045–2049, 2011.
23. Rovers, J., J. Jansen, J. Compter, and E. Lomonova, "Analysis method of the dynamic force and torque distribution in the magnet array of a commutated magnetically levitated planar actuator," *IEEE Transactions on Industrial Electronics*, Vol. 59, No. 5, 2157–2166, May 2012.
24. Allag, H., J.-P. Yonnet, M. Fassenet, and M. E. H. Latrech, "3D analytical calculation of interactions between perpendicularly magnetized magnets — Application to any magnetization direction," *Sensors Letters*, Vol. 7, No. 3, 1–6, June 2009.
25. Allag, H. and J.-P. Yonnet, "3-D analytical calculation of the torque and force exerted between two cuboidal magnets," *IEEE Transactions on Magnetics*, Vol. 45, No. 10, 3969–3972, October 2009.
26. Yonnet, J. P., H. Allag, and M. E. H. Latrech, "2D and 3D analytical calculations of magnet interactions," *Proc. MmdE Conf.*, Bucharest, June 15–16, 2008.
27. Xu, F., X. Xu, Z. Li, and L. Chu, "Numerical calculation of the magnetic field and force in cylindrical single-axis," *IEEE Transactions on Magnetics*, Vol. 50, 1–6, 2014.
28. Wang, Z. and Y. Ren, "Magnetic force and torque calculation between circular coils with nonparallel axes," *IEEE Transactions on Applied Superconductivity*, Vol. 24, No. 4, 4901505, 2014.